Tunable nanophotonic delay lines using linearly chirped contradirectional couplers with uniform Bragg gratings

Wei Shi,[1,2,*] Venkat Veerasubramanian,[1] David Patel,[1] and David V. Plant[1]

[1]*Department of Electrical and Computer Engineering, McGill University, Montreal, Quebec, Canada*

[2]*Currently with the Department of Electrical and Computer Engineering, Université Laval, Québec City, Quebec, Canada*

**Corresponding author: wei.shi3@mcgill.ca*

Received August 21, 2013; revised November 17, 2013; accepted December 10, 2013; posted December 23, 2013 (Doc. ID 196180); published January 30, 2014

We demonstrate an integrated tunable optical delay line in grating-assisted contradirectional couplers using a CMOS-compatible photonic technology. The input signal is delayed through dispersive Bragg gratings and distributedly coupled to the drop port of the coupler without backreflections. This add–drop design enables monolithic integration of grating-based delay lines without using optical circulators. The gratings are formed by slab perturbations in rib waveguides, with the index chirping realized by linearly tapering the rib widths. Both the pitch and size of the gratings are constant through the entire coupler, for a higher tolerance to fabrication errors. Continuous tuning of the optical group delay of up to 96 ps has been obtained, with a low insertion loss of less than 2 dB and a negative chromatic dispersion of −11 ps/nm that allows for bit rates of up to almost 100 Gb/s at the maximal delay. The device has a small footprint of 0.015 mm^2, and can be used for on-chip optical buffering, dispersion compensation, and pulse compression.

OCIS codes: (130.2035) Dispersion compensation devices; (200.4490) Optical buffers; (250.5300) Photonic integrated circuits.

http://dx.doi.org/10.1364/OL.39.000701

Tunable optical delay lines are widely used in optical communications for dispersion compensation [1] and optical signal processing [2]. While they are conventionally implemented using chirped fiber Bragg gratings [1], there has been significant interest in realizing integrated tunable delay lines, especially on a silicon-on-insulator (SOI) platform, for on-chip optical interconnects [3,4]. Various solutions based on microring resonators and photonic crystals have been exploited, showing large delays and high tunability [4,5]. However, they suffer from high losses, typically 35 to 100 dB/ns [3–5], which is a major obstacle to their adoption in systems. Chirped waveguide Bragg gratings have low losses (<10 dB/ns) [6], and thus are attractive for photonic integrated circuits without optical amplification. A continuously tunable delay line using linearly chirped Bragg gratings was recently demonstrated in micrometer-scale SOI waveguides [7]. Realization of nanophotonic Bragg-grating devices is important for their applications in large-scale integrated photonic circuits [8–10], because most CMOS-compatible active components, such as high-speed optical modulators and detectors, are developed on nanometer-scale (e.g., 220 nm) SOI wafers [11].

In this Letter, we demonstrate a continuously tunable delay line, using grating-assisted contradirectional couplers (contra-DCs), on a 220 nm high SOI wafer. This design has the inherent merit of add–drop (i.e., 4-port) operation [12], circumventing the need for optical circulators, and thus can be easily integrated monolithically. Continuous index variation is obtained by waveguide tapering for a chirped design with uniform Bragg gratings. First-order silicon Bragg gratings have pitches of only a few hundred nanometers. This leads to compact devices but also makes the fine tuning of grating pitches challenging. While discrete delay tuning can be obtained by stepped pitch variation [10], it is easier to taper waveguide widths for continuous tuning [7]. The use of uniform gratings ensures that lithography effects are constant throughout the coupler, and thus can be more precisely predicted [13].

The schematic of the proposed device is shown in Fig. 1. It consists of two different-sized rib waveguides with a series of dielectric perturbations (i.e., holes) on the slab in between. This slab-modulated structure [14] enables flexible apodization or chirping designs by shaping the waveguide geometry without fine tuning small perturbation features, producing a design with high reliability. Based on this scheme, a novel coupler-apodized Bragg grating add–drop filter was demonstrated using

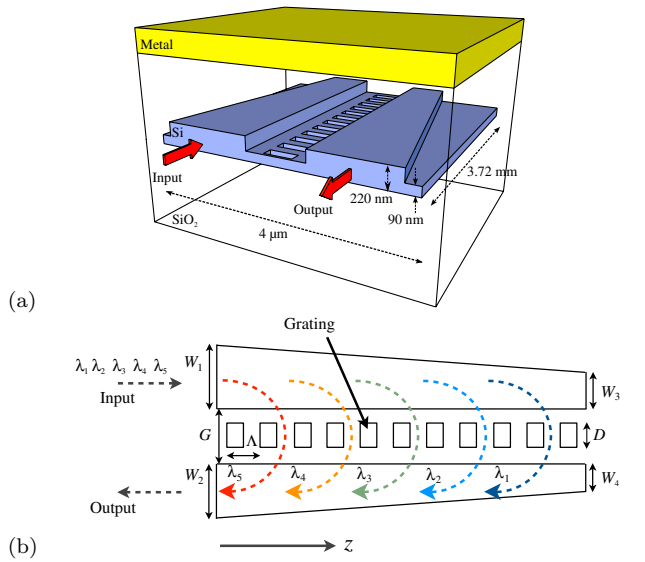

Fig. 1. Schematic of the tunable optical delay line using contra-DCs in rib waveguides with uniform Bragg gratings: (a) perspective view and (b) top view.

193 nm lithography, showing high sidelobe suppression of 30 dB [13]. Here, we keep the grating uniform (i.e., both the size and pitch of the perturbations are constant throughout the entire coupler), and taper the waveguides for index chirping. With the assistance of the grating, the optical input is coupled backward to the output waveguide. The central wavelength of this contradirectional coupling is a function of position (z), determined by the phase-matching condition [12] $\lambda_c(z) = \Lambda[n_1(z) + n_2(z)]$, where $n_1(z)$ and $n_2(z)$ are local effective indices of the supermodes coupled to each other. As the waveguides taper down along the coupler, the phase-matching condition shifts to shorter wavelengths. Therefore, various wavelengths travel different distances with distinct delays before being dropped to the output. For a fixed wavelength, we can change the effective indices, e.g., by the thermo-optic effect, and thus the position that satisfies the phase-matching condition for the delay tuning.

The device is designed for transverse electric polarization with parameters described as follows. The rib waveguides are 220 nm high with a 90 nm slab, sitting on a 3 μm buried oxide layer, covered by a 2 μm SiO_2 cladding. As illustrated by Fig. 1(b), the ribs are linearly tapered from 620 nm (W_1) and 420 nm (W_2) to 600 nm (W_3) and 400 nm (W_4), respectively. Therefore, the two waveguides have a constant difference of 200 nm in width. This high asymmetry results in very weak codirectional coupling, which is important for suppressing backreflections and phase noise [12]. Other parameters include a uniform pitch Λ of 310 nm, a coupler gap G of 600 nm, and a perturbation width D of 300 nm, which are all constant through the entire coupler for a uniform grating design. The entire coupler is 3.72 mm in length and 4 μm in width, giving a small footprint of 0.015 mm^2. Using coupled-mode theory and the transfer-matrix method [12], the transmission and group delay τ are calculated and shown in Fig. 2. Within the passband, the delay and the loss increase as the wavelength decreases due to the increased propagation distance.

The device with the parameters just described was fabricated using e-beam lithography. A 300 nm thick, 5 μm wide aluminum strip was deposited on top of the oxide cladding for thermal tuning, with a resistance measured as 270 Ω. The transmission spectrum, as shown in Fig. 3, was measured using fiber-grating couplers (FGCs) and was normalized to the response of a pair of FGCs. The

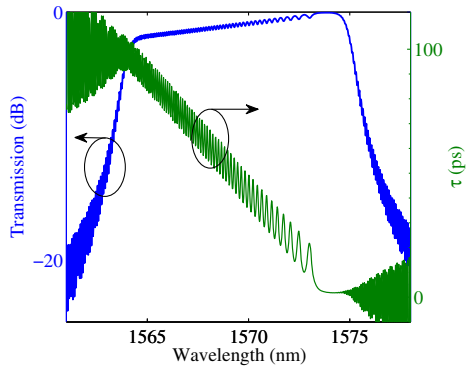

Fig. 2. Calculated transmission and group delay of the proposed photonic delay line.

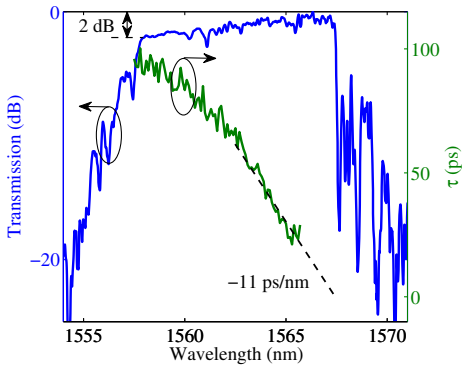

Fig. 3. Measured transmission and group delay of the proposed photonic delay line.

group delay was measured by characterizing the waveforms generated by an external modulator with non return-to-zero (NRZ) signals operating at 10 Gb/s, similar to the method used in [3,10]. The passband is 9.5 nm wide. The excess loss near the band edge at the short-wavelength side (1558 nm) is less than 2 dB, corresponding to the total loss though a round trip (7.44 mm) of the entire coupler, by which a propagation loss of 2.7 dB/cm is extracted. The range of the delay measurement was limited by the bandwidth of the EDFA used for compensating for the insertion losses of the FGCs and the modulator. A delay of 96 ps was measured at 1558 nm, by which an average group index of 3.87 is extracted. Ripples are observed in both the transmission and delay spectra, which can be suppressed by grating apodization. All these results agree well with the simulation.

The delay has a slope of −11 ps/nm, indicating a negative chromatic dispersion D of −3 ps/(nm · mm). While the maximal bit rate $B_{\max}$ depends on modulation formats and receiver design, the chromatic dispersion limit can be estimated for NRZ pulses by [15]

$$B_{\max}(\text{in Gb/s}) = \sqrt{\frac{10^5}{|D| \cdot L}}, \tag{1}$$

where L is the dispersive waveguide length and equals 3.72 mm for the maximal delay, which results in a bit rate of greater than 95 Gb/s for 96 ps of delay. Higher bit rates are feasible for lower delays. Improved system performance is anticipated when this device is used together with other components that have positive dispersions (e.g., optical fibers). Specifically, this device is able to compensate for the dispersion induced by a 647 m long standard single-mode optical fiber with a chromatic dispersion of 17 ps/(nm · km). The negative dispersion can also be used for on-chip pulse compression [16].

The measured spectrum shows a blue shift of about 6 nm compared to the simulation, which is due to fabrication errors such as wafer nonuniformity and waveguide width variations [8]. The fabrication errors may also cause phase noise [9], which results in stronger sidelobes and spectral shape distortion. The loss per unit delay is 20 dB/ns, higher than that of micrometer-scale Bragg gratings [7] due to stronger sidewall scatterings. Recent progress in SOI waveguides has shown very

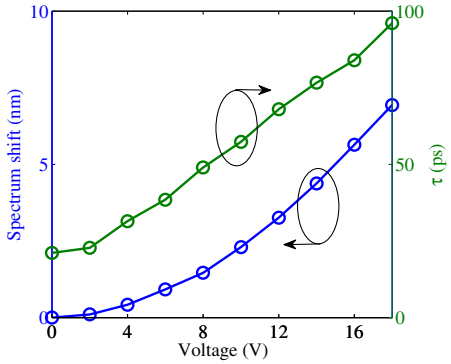

Fig. 4. Measured spectrum shift and group delay at 1565.3 nm, as a function of the applied voltage.

low losses of below 0.1 dB/cm [17], which may lead to a significantly reduced loss per unit delay of below 1 dB/ns.

The device was electrically probed and tuned. The measured results with a fixed wavelength of 1565.3 nm are shown in Fig. 4. As the voltage increases, the spectrum red shifts and, accordingly, the group delay increases. Continuous delay tuning, from 21 to 96 ps, has been obtained with the spectrum shifted over 7 nm. A delay below 21 ps is also feasible but was not measured, again, due to the bandwidth of the EDFA. Assuming a typical thermal tuning coefficient 0.09 nm/K, the local temperate on the chip is estimated to be increased by 78 K for the maximum delay, leading to a thermal tuning coefficient of 1 ps/K. For proof of concept, a simple, bulky metal heater was used to cover a large area, which resulted in a relatively low power efficiency of about 11 mW/ps. It can be significantly improved by optimizing the heater design with a smaller feature size and a suspended waveguide structure [18].

In summary, we have proposed and demonstrated a tunable group delay line using silicon nanophotonic contra-DCs. Linear index chirping is realized by waveguide tapers with uniform Bragg gratings, which circumvents the need for fine tuning of small grating features for a higher tolerance to fabrication errors. Continuous tuning of group delay up to 96 ps has been achieved with a low insertion loss of less than 2 dB. A negative chromatic dispersion of −11 ps/nm has been achieved for a 3.72 mm long, 4 μm wide device. In comparison with the delay lines using photonic crystals and microring resonators [4,5], our device shows a lower insertion loss and a comparable footprint (0.015 mm^2 vs. ~0.025 mm^2 [4,5]). In addition, our device is attractive due to the simplicity in fabrication and tuning, while photonic crystals are challenging in implementation using optical lithography and cascaded microrings have a stringent requirement for resonance alignment. Operating in the drop mode with no or very weak backreflections, this device can easily be integrated with other photonic components for on-chip applications, such as interconnects, signal processing, and pulse compression.

We thank H. Yun, J. Flueckiger, and L. Chrostowski at the University of British Columbia for the PDK and assistance, and E. Huante-Ceron and A. Knights at McMaster University for the metallization. The devices were fabricated at the University of Washington Microfabrication/Nanotechnology User Facility, a member of the NSF National Nanotechnology Infrastructure Network.

References

1. Y. Painchaud, C. Paquet, and M. Guy, Opt. Photon. News **18**(9), 48 (2007).
2. J. Yao, IEEE Photon. Soc. Newslett. **26**(3), 5 (2012).
3. F. Xia, L. Sekaric, and Y. Vlasov, Nat. Photonics **1**, 65 (2007).
4. A. Melloni, A. Canciamilla, C. Ferrari, F. Morichetti, L. O'Faolain, T. Krauss, R. De La Rue, A. Samarelli, and M. Sorel, IEEE Photon. J. **2**, 181 (2010).
5. P. A. Morton, J. Cardenas, J. B. Khurgin, and M. Lipson, IEEE Photon. Technol. Lett. **24**, 512 (2012).
6. S. Khan, M. A. Baghban, and S. Fathpour, Opt. Express **19**, 11780 (2011).
7. I. Giuntoni, D. Stolarek, D. I. Kroushkov, J. Bruns, L. Zimmermann, B. Tillack, and K. Petermann, Opt. Express **20**, 11241 (2012).
8. X. Wang, W. Shi, H. Yun, S. Grist, N. A. F. Jaeger, and L. Chrostowski, Opt. Express **20**, 15547 (2012).
9. A. D. Simard, N. Belhadj, Y. Painchaud, and S. LaRochelle, IEEE Photon. Technol. Lett. **24**, 1033 (2012).
10. M. Spasojevic and L. R. Chen, Electron. Lett. **49**, 608 (2013).
11. G. T. Reed, G. Mashanovich, F. Y. Gardes, and D. J. Thomson, Nat. Photonics **4**, 518 (2010).
12. W. Shi, X. Wang, C. Lin, H. Yun, Y. Liu, T. Baehr-Jones, M. Hochberg, N. A. F. Jaeger, and L. Chrostowski, Opt. Express **21**, 3633 (2013).
13. W. Shi, H. Yun, C. Lin, J. Flueckiger, N. A. F. Jaeger, and L. Chrostowski, Opt. Lett. **38**, 3068 (2013).
14. W. Shi, X. Wang, W. Zhang, L. Chrostowski, and N. A. F. Jaeger, Opt. Lett. **36**, 3999 (2011).
15. I. Kaminow and T. Li, *Optical Fiber Telecommunications IV-B: Systems and Impairments* (Academic, 2002).
16. D. T. H. Tan, P. Sun, and Y. Fainman, Nat. Commun. **1**, 116 (2010).
17. W. Bogaerts and S. Selvaraja, IEEE Photon. J. **3**, 422 (2011).
18. P. Dong, W. Qian, H. Liang, R. Shafiiha, D. Feng, G. Li, J. E. Cunningham, A. V. Krishnamoorthy, and M. Asghari, Opt. Express **18**, 20298 (2010).